J. Indian Inst. Sci., July–Aug. 1988, **68**, pp. 277–294.

Role of crystallography in understanding reactions in the solid state*

H. MANOHAR
Department of Inorganic and Physical Chemistry, Indian Institute of Science, Bangalore 560 012, India.

Received on March 24, 1988; Revised on May 24, 1988.

Abstract

In recent years, X-ray crystallography has been extensively employed to study solid-state reactions. It is found that the initiation and progress of many of these reactions is governed by structural and geometric factors. Such reactions are known as topochemical reactions. While, in general, solid-state reactions take place in polycrystalline samples, some are known to occur in single crystals without a breakdown of the lattice. The reason for this is the close similarity in the reactant and product structures. These reactions are termed topotactic reactions. In this brief review, a few examples of topochemical and topotactic reactions are discussed, and the important role of crystallography in elucidating their mechanism highlighted.

Key words: Solid-state reactions, topochemical reaction, topotactic reaction, X-ray crystallography, reaction mechanism.

1. Introduction

In recent years, there has been an upsurge of interest in the study of solid-state reactions. While a variety of sophisticated experimental techniques like thermo-analytical techniques, spectroscopy, high-resolution electron microscopy, etc., have been employed, X-ray crystallography has been found to be a potent tool to understand the mechanism of the reaction at the atomic or molecular level.

It is now realised that the initiation and progress of many solid-state reactions is governed by the constraints imposed by the crystal lattice, where atoms and molecules are located in relatively fixed positions. Consequently, structural and geometric parameters such as packing and orientation of the reactant molecules, conformation of substituent groups, short contacts between potentially reacting centres play a very significant role, in contrast to electronic and dipolar effects which are important in reactions occurring in solution. This leads, sometimes, to formation of products which are difficult or

*Updated version of an invited talk delivered at the XVIII National Seminar on Crystallography, Jammu, Oct. 1986.

virtually impossible to prepare by conventional methods. In some cases the rate of the reaction in the solid is much faster than in solution, a fact which is not easy to comprehend. These reactions are known as topochemical reactions. Many organic solid-state reactions, thermally induced as well as photochemical, have been identified to be topochemically controlled.

Generally solid-state reactions take place in microcrystalline (powdered) samples. However, some reactions are known to occur in single crystals; *i.e.*, a single crystal of the reactant is converted into a single crystal of the product as a pseudo-morph, without change in external shape. The conversion takes place in the entire volume of the crystal and there exist certain definite three-dimensional orientation relationships between the reactant and product lattices. The reason why there is no break up of the lattice in such cases is due to small or negligible movement of atoms about lattice points because of close similarity or a relationship between the respective structures. (Some cases are known where the product is not exactly a single crystal, but an aggregate of micro-crystallites oriented in certain preferred directions. Even here it has been possible to determine the orientation relationships). Such reactions are termed as topotactic reactions[1]. Topotaxy has been observed in a variety of reactions such as polymorphic transformations, oxidations, dehydrations, decompositions, etc., both in inorganic as well as organic compounds. In this brief review, a few representative examples of topochemical and topotactic reactions, including work done in the author's laboratory, will be presented. It will be shown how these studies have thrown light on the mechanisms of the reactions. It may be added here that the choice of examples is necessarily dictated by the author's own personal preferences and his research interests. Excellent reviews on both the topics are available in the literature (see, for example, references 2–10 for topochemical reactions and 11–17 for topotactic reactions).

2. Topochemical principles

Pioneering work in the area of topochemical reactions was done by Gerhardt Schmidt in the 1950s and 1960s on the photodimerization of substituted cinnamic acids to give cyclobutane derivatives[18]. While in solution, the trans-cinnamic acids are either photoinactive or yield mixtures of various possible stereo-isomers, in the solid state stereospecific products were obtained depending on the crystal packing. Based on these results he enunciated the topochemical principles governing such reactions:

Reactions in the solid state occur with a minimum of atomic or molecular movements and are thus governed by the structures of the starting materials. For the reaction to occur, potentially reacting centres must be suitably oriented with a separation of not more than *ca.* 4.2 Å (This figure was arrived at on the basis of a number of experimental results).

These principles have been very useful in predicting and understanding the course of many solid-state reactions. Attention has subsequently shifted to the control of crystal structures and a new branch of the subject, 'crystal engineering', which is concerned with trying to obtain topochemical control in systematic ways has come into being[2]. Again the

possibility of accomplishing asymmetric syntheses by performing solid-state reactions on molecules which are optically inactive in solution, but which form chiral single crystals has opened up new perspectives in organic chemistry[19,20]. However, we will not go into these exciting developments which are outside the scope of this paper.

3. Thermally induced acyl migration from *O*- to N-position in salicylamides

O-acetyl salicylamide(Ia) is known to rearrange irreversibly to N-acetyl salicylamide(IIa) under a variety of conditions, both in solution and in the solid state (Scheme I). The reaction was studied earlier by spectroscopic as well as thermoanalytical techniques[21], but no crystallographic work has been done. We decided to examine the crystal structures to see if they can throw some light on this interesting reaction. Subsequently the work was extended to the benzoyl(b) and propionyl(c) derivatives.

The crystal structures of the reactants as well as products in all the three cases have been solved[22,23]. The molecular structure of I(a) is shown in fig. 1. The reaction may be viewed as a nucleophilic addition at the carbonyl carbon atom, C(8), the nucleophile being the amide nitrogen, N(1), with a lone pair of electrons[24]. The main step in the reaction is the bond formation between C(8) and N(1). Therefore, according to the topochemical principles, the following parameters in the reactant molecules are of relevance: (i) Conformations of the amide and acyl groups, which should be such that the reacting centres are suitably aligned to favour the reaction; (ii) The contact distance C(8)...N(1), which should be favourable for bond formation; (iii) The angle N(1)...C(8)–O(3), (α), representing the direction of the nucleophile, which should be *ca.* 109°; (iv) The angle C(7)–N(1)...C(8), (α'), which should be *ca* 90°, if the lone pair on N(1) points towards C(8). These parameters, both in the intramolecular as well as intermolecular case, for compounds Ia, Ib and Ic, are given in Tables I and II.

In the case of I(a), both the inter- as well as intramolecular contacts are within the range in which topochemical criteria apply; however, the intramolecular distance is the shortest. This fact, together with a consideration of the values of the corresponding angles, α and α', suggests that an intramolecular mechanism is favoured. In the other two cases, I(b) and I(c), however, there is stronger support for this mechanism, as the intermolecular contacts are all greater than 5.0 Å. It may be added that the product structures (IIa, b and c) are quite different and apparently do not play any role in the reaction.

4. Methyl migration in methyl *p*-dimethylaminobenzenesulphonate

It was reported that solutions of methyl *p*-dimethylaminobenzenesulphonate (MSE) in a variety of solvents remained unchanged on standing at room temperature even for months[25]. However, in the solid under these conditions or more rapidly at higher temperatures, MSE was cleanly converted to *p*-trimethylammonium benzene sulphonate zwitterion (ZWT) (Scheme II). Another interesting feature was that the rate of the re-

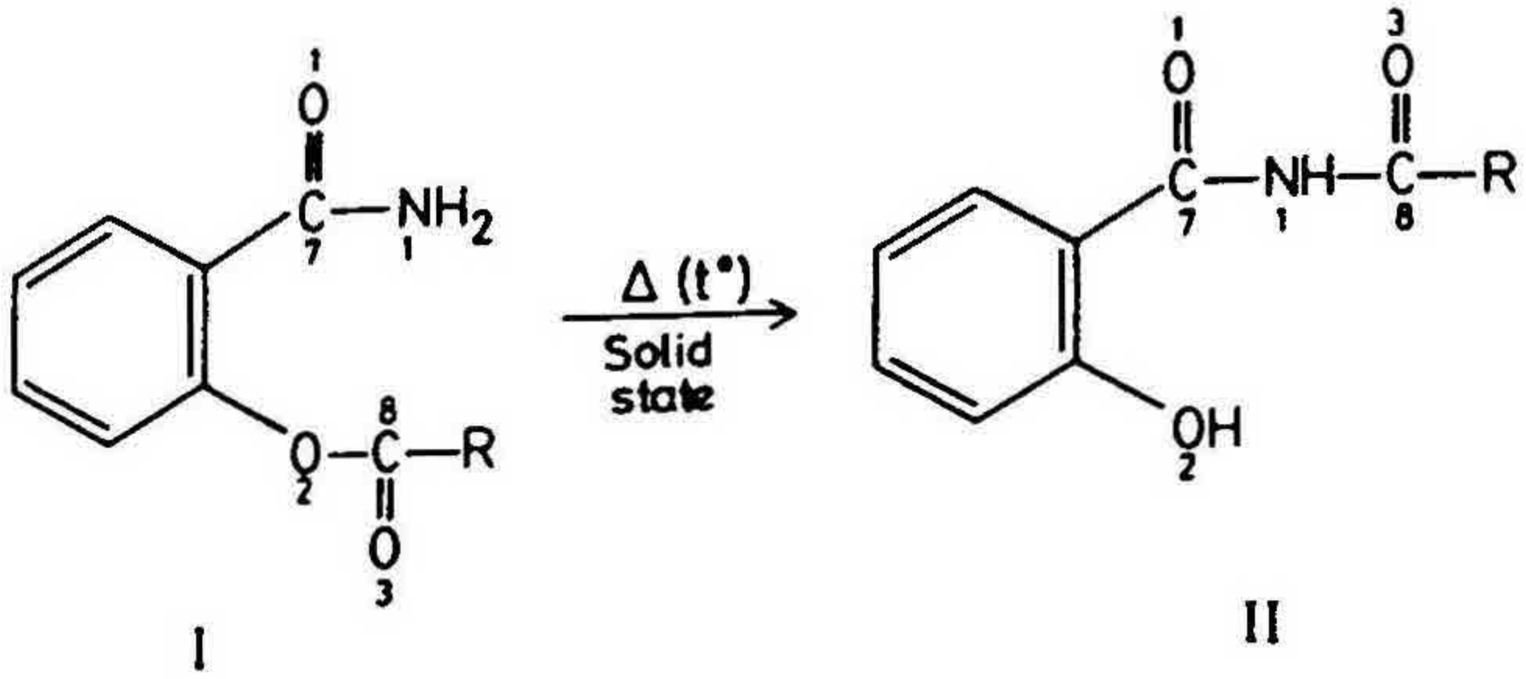

(a) R = CH_3, t ~ 100°C; (b) R = C_6H_5, t ~ 120°C; (c) R = C_2H_5, t ~ 85°C.

Scheme I

arrangement studied by NMR, increases at higher temperatures, but this is true only for temperatures below the melting point of MSE. Melting introduces a sharp decrease in the rate of conversion. It was found that the crystal reacts 25 to 40 times faster than the melt.

There are two general mechanisms for this interesting reaction. One is a simple intramolecular shift of the ester methyl to the dimethylamino group. While this is a straightforward process, it would involve very severe molecular distortion. The other alternative is an intermolecular chain reaction or at least a dimeric process or some variation on this intermolecular theme. This basic question was answered by Bergmann and coworkers by a 'double label scrambling experiment' using field desorption mass spectrometry. The

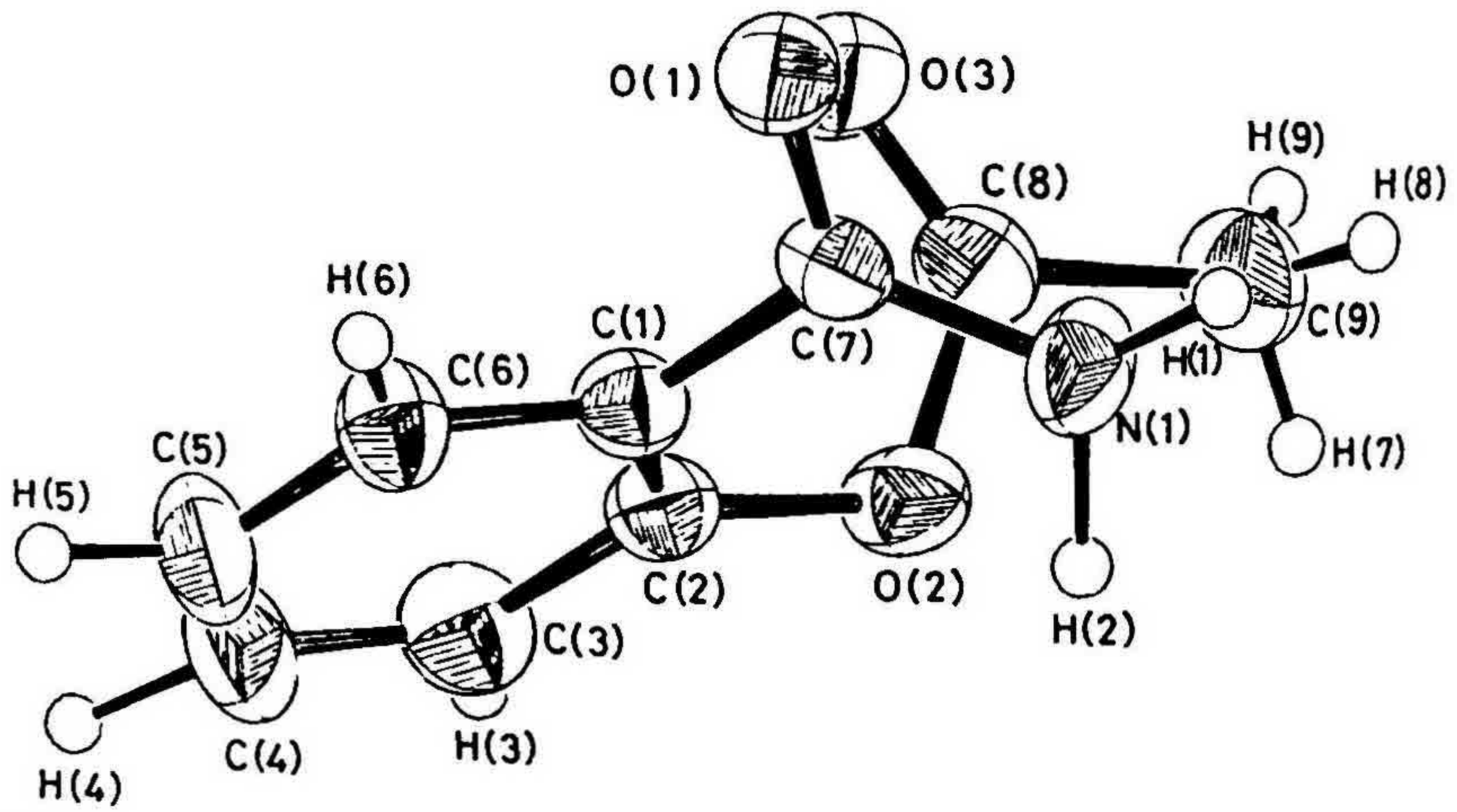

FIG. 1. Molecular structure of *O*-acetyl salicylamide, I(a) (reprinted from ref. 23 with permission).

Table I
Dihedral angles (°) of substituent groups with the benzene ring in *O*-acylsalicylamides

	I(a)	I(b)	I(c)
Amide group ($-CONH_2$)	39.9	37.9	32.2
Acyl group ($-COR$)	78.1	93.4	93.3

Table II
Structural parameters in *O*-acylsalicylamides[22]

	I(a)	I(b)	I(c)
Intramolecular			
C(8)...N(1) (Å)	3.27	3.53	3.34
α(°)	101.7	116.1	110.6
α'(°)	81.1	79.4	86.5
Intermolecular			
C(8)...N(1) (Å)	3.88, 3.91	—	—
α(°)	132.5, 68.4	—	—
α'(°)	111.0, 106.0	—	—

results indicated the intermolecularity of the reaction. Conclusive proof for this mechanism was provided by the crystal structure of MSE.

A view of the stacking along one chain of molecules in the crystal perpendicular to the (101) plane (fig. 2) is very revealing. The molecules stack with alternating dimethylamino and sulfonate groups one exactly above the other and with aromatic rings inclined *ca.* 76° to each other. Each nitrogen is in alignment with a sulfonate ester methyl group; N...C is only 3.54 Å and O(1)–C(9)...N angle is 147°, close to the linear arrangement required for nucleophilic substitution in a bimolecular reaction. The system can, therefore, readily transfer each ester methyl group to its neighbouring N atom. Thus the packing of the molecules in the crystal and the relative orientation of the reactive sites are such as to facilitate the proposed chain-reaction mechanism. This result may be contrasted with the previous case, where an intramolecular mechanism was proposed.

5. Photochemical oxidation of thioketones in the crystalline state

The above two are examples of thermally induced rearrangements. We will next deal with a photochemically induced oxidation reaction.

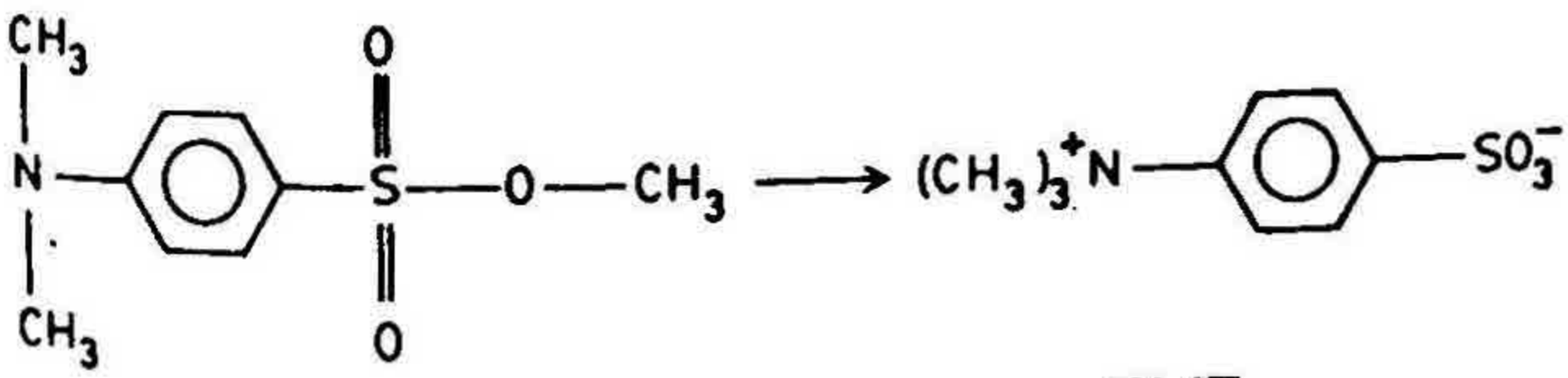

Scheme II

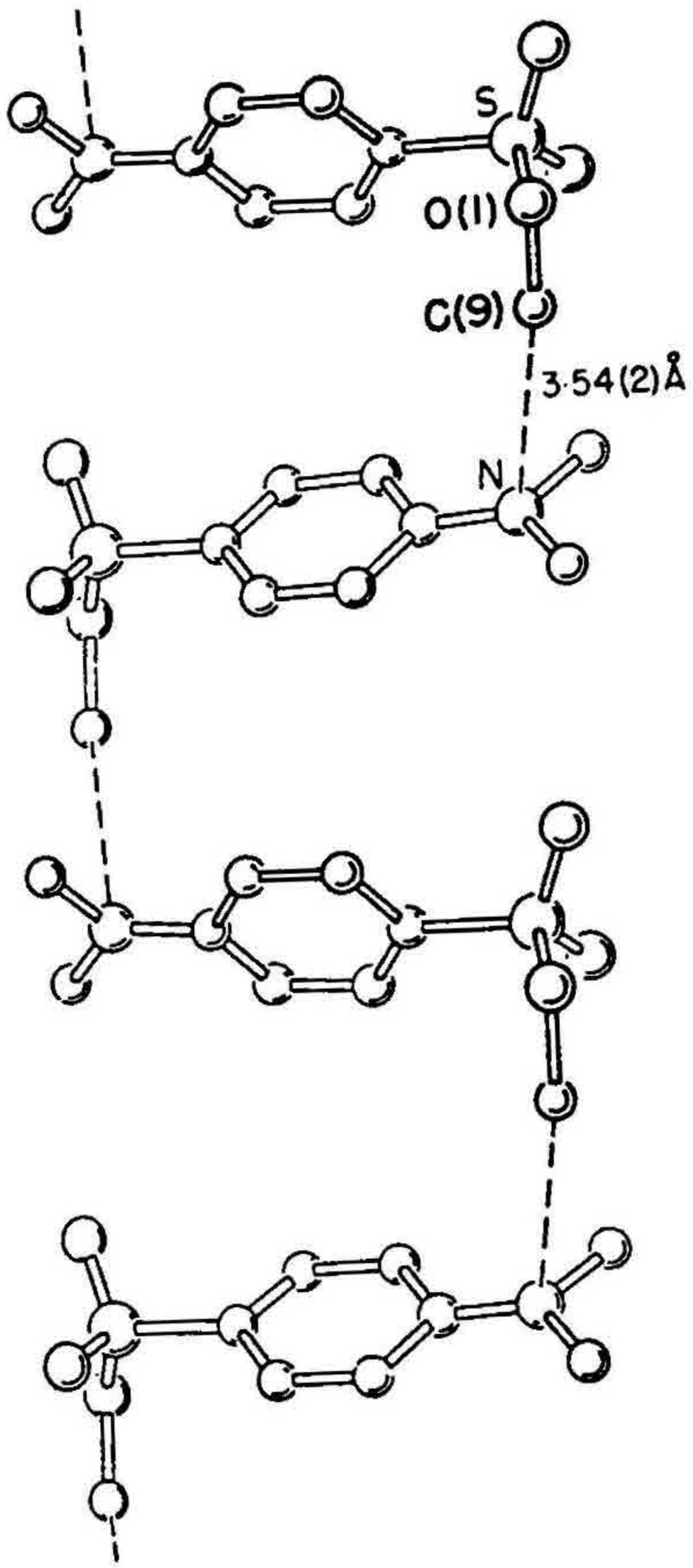

FIG. 2. A view of the stacking along one chain of molecules in crystals of methyl *p*-dimethylaminobenzenesulphonate (MSE), as seen perpendicular to (101) plane (reprinted from ref. 25 with permission).

Thioketones, in general, are readily oxidized in solution to the corresponding S-oxides and/or ketones upon exposure to visible light. The rate and product distribution of oxidation are controlled by their inherent electronic and steric properties. However, in the crystalline state, among the large number of diaryl thioketones investigated by Arjunan *et al* only a few underwent photo-oxidation[26]. For example, in Table III, while 4,4'-dimethoxythiobenzophenone (5) is most reactive in solution, surprisingly, it is stable in the

Table III
Photooxidation of some diaryl thioketones in the solid state and their crystal properties[26]

Crystal studied	Duration of irradiation (days)	Nature of reaction		Crystal data	Channel axis	Cross-sectional area of channel ($Å^2$)
		in solution	in solid state			
(1)	1	Yes	Yes	$P2_1/n$, $a=14.042$, $b=5.863$, $c=13.402$ Å, $\beta=106.4°$, $Z=4$	b	9
(5)	30	Yes	No	PI, $a=9.810$, $b=9.635$, $c=15.015$ Å, $\alpha=79.11$, $\beta=102.30$, $\gamma=107.76°$, $Z=4$		
(6)	30	Yes	No	$P2_1/c$, $a=17.029$, $b=6.706$, $c=14.629$ Å, $\beta=113.5°$, $Z=4$	b	2.3
(7)	17	Yes	Yes	$P2_12_12_1$, $a=5.873$, $b=13.677$, $c=15.668$ Å, $Z=4$	a	8.3

crystal. Single crystal X-ray analyses of some of the thioketones were, therefore, undertaken and an attempt was made to understand the reactivity patterns of these compounds in terms of their molecular packing. Four of the thioketones investigated are shown in fig. 3 and their crystal properties are tabulated in Table III (the X-ray structure of 1 had been solved earlier). Of these four, 1 and 7 are photo-oxidisable while 5 and 6 are inert.

A comparison of the molecular packing of the thioketones (figs 4 and 5) is quite revealing in rationalising their photo-reactivity in the solid state. It may be observed from fig. 4, that in reactive thioketones there is a channel along the shortest crystallographic axis with the thiocarbonyl chromophore directed along the channel. Further, the S...S intermolecular distances between adjacent planes in all these cases are < 3.9 Å. On the other hand, in the case of stable thioketones (fig. 5), the packing arrangement does not reveal such a channel along any of the crystallographic axes. Further, the S...S contact distances between adjacent layers are 4.83 and 6.05 Å for 5 and 6, respectively, much larger than in reactive thioketones. Thus it may be hypothesized that the channel is

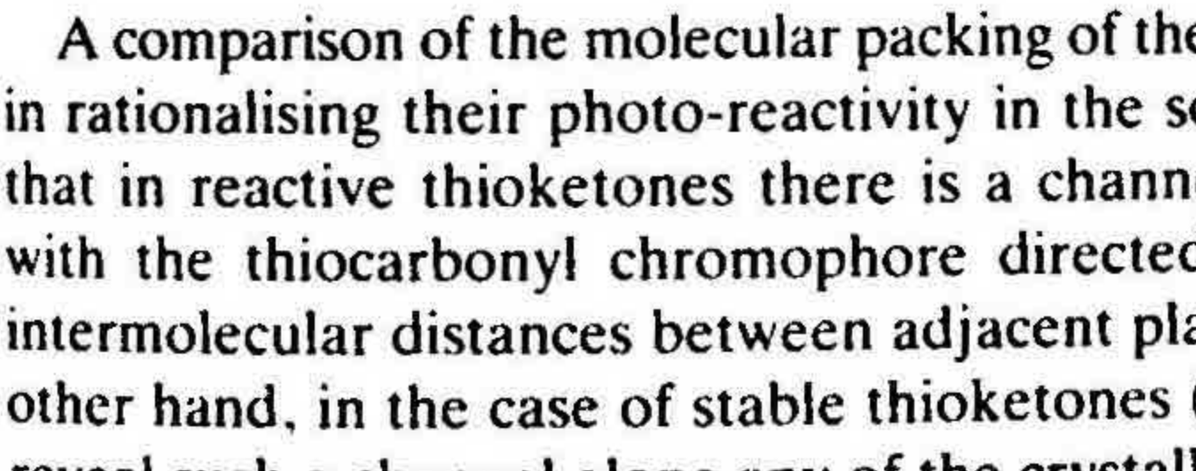

1: R = R' = H; 5: R = R' = OCH_3; 6: R = $N(CH_3)_2$

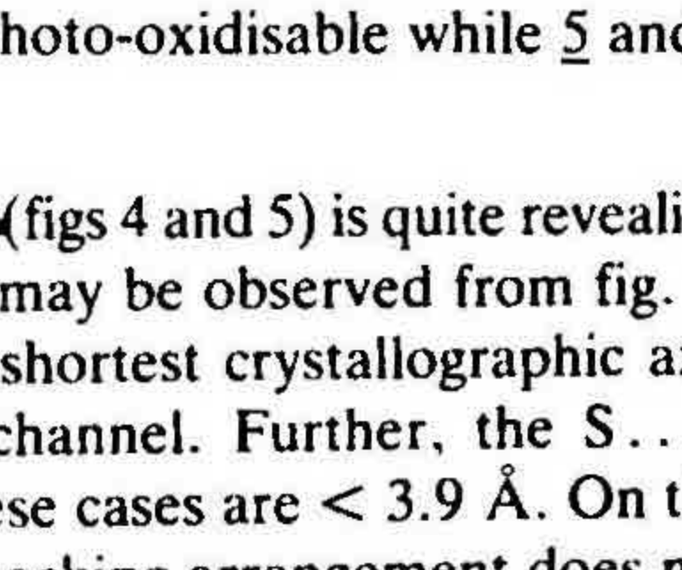

7

FIG. 3. Some thioketones investigated in the solid state (reprinted from ref. 26 with permission).

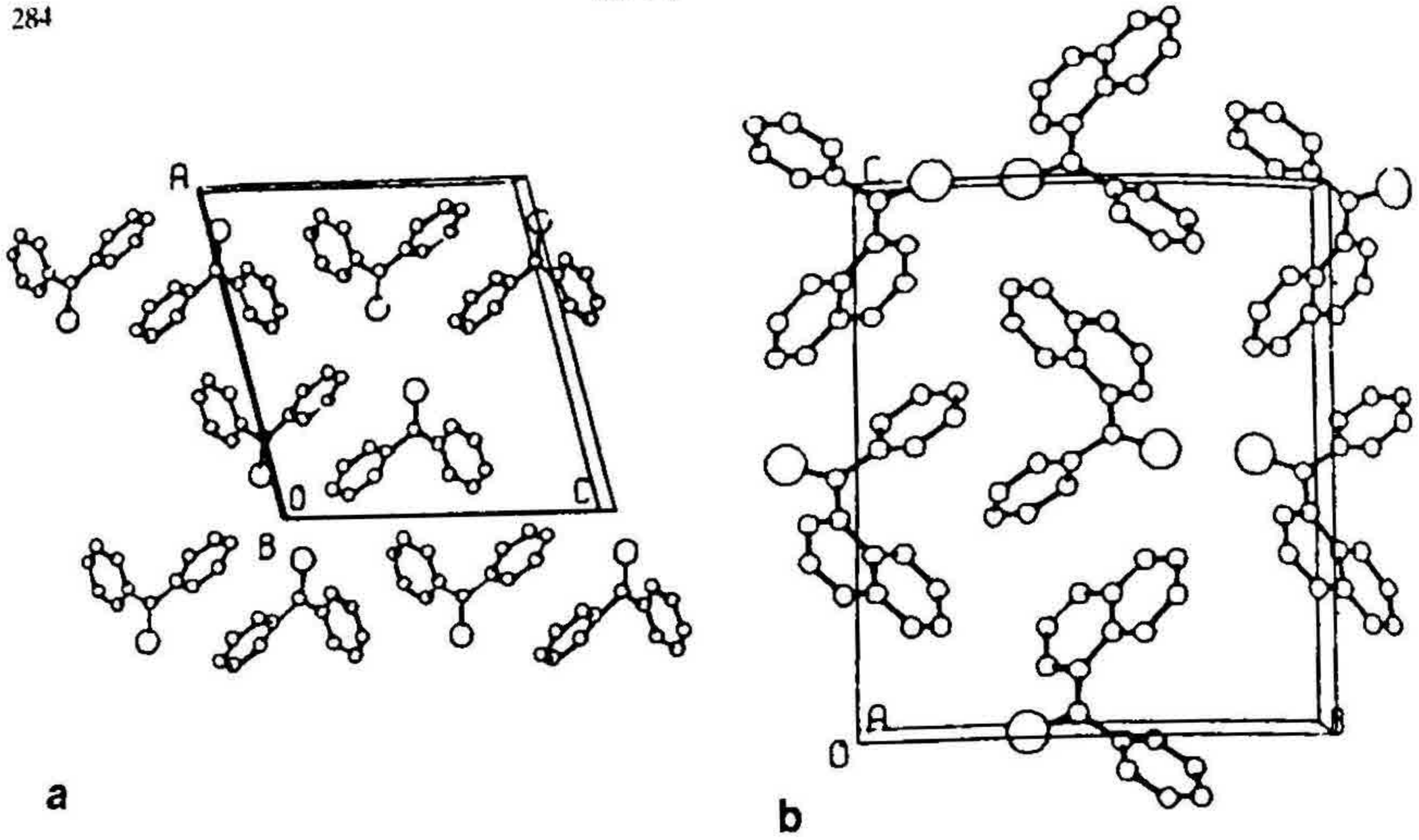

FIG. 4. The molecular crystal packing of reactive thioketones, 1 and 7. (a) 1, view along *b* axis, (b) 7, view along *a* axis (reprinted from ref. 26 with permission).

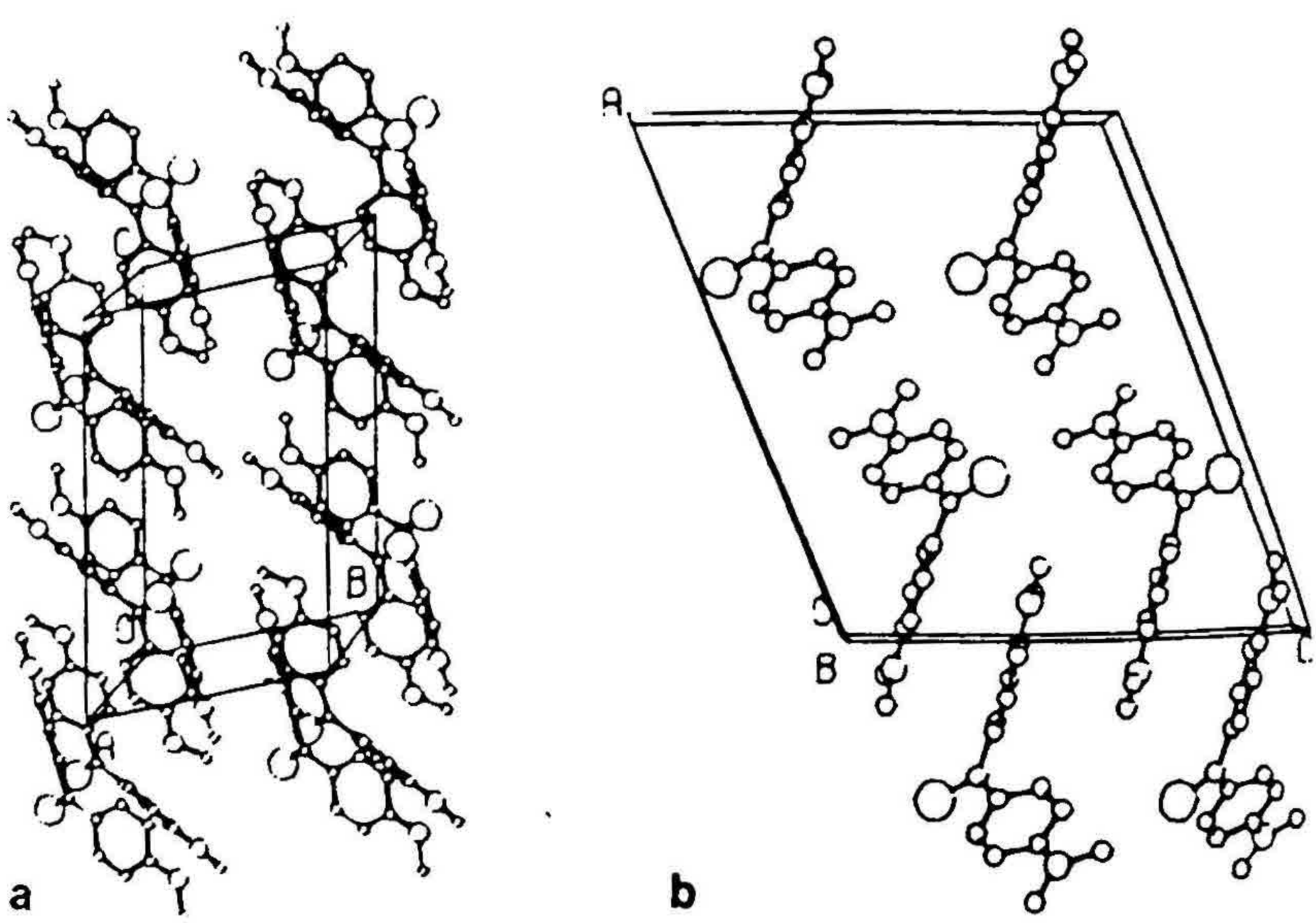

FIG. 5. The molecular crystal packing of unreactive thioketones (5 and 6). (a) 5, view along *a* axis. (b) 6, view along *b* axis (reprinted with permission from ref. 26).

essential for oxygen to diffuse into the crystal and effect oxidation. The cross-sectional areas of the channels were next calculated (Table III). For the unreactive thioketones, 5 and 6, there is either no channel (5) or it is too small (≈ 2.3 Å for 6). On the other hand, for the reactive thioketones, 1 and 7, the channel cross-sectional area is fairly large (> 8.3 Å). From the nature of the packing modes it was also anticipated that the reaction is initiated on (010) and (100) faces for (1) and (7) respectively.

On the basis of the above results a simple mechanism has been proposed for the oxidation of thioketones in the solid state[26]. This involves attack of oxygen at the exposed excited-thiocarbonyl chromophore at the crystal surface to form a monolayer of the carbonyl compound. A disorientation of the reacted layer takes place so as to allow the oxygen to diffuse into the next layer where the process is repeated. Thus, apart from the requirement of a thiocarbonyl chromophore at the crystal surface, it is also necessary that the thiocarbonyl groups are so arranged that the oxidation of one molecule exposes another close neighbour to an oxygen molecule.

There are several examples of solid-state reactions which seemingly contravene topochemical principles[27]. For example, in some reactant crystal structures, dimers are formed even though the molecules do not approach to within the critical distance necessary for photodimerisation. Sometimes products other than those predicted by topochemical arguments are formed. We will not go into the details here, except to point out that the general consensus is that structural imperfections play a dominant role in these non-topochemical reactions.

6. Early work on topotactic reactions

Pioneering work was done by Bernal and coworkers in the 1950s in the iron oxide system[28,29]. For example, wustite(FeO), magnetite(Fe_3O_4), and maghemite (γ-Fe_2O_3), all of which have structures based on cubic-close packing of oxide ions, can be inter-converted by heating in suitable atmospheres. X-ray studies showed that the directions of the crystallographic axes in these oxides do not change during the reactions, which proceed by addition or removal of oxygen layers and appropriate migration of cations. Considerable work has also been done on the hydroxides, oxide hydroxides and silicates of small cations like iron, aluminium and magnesium[30]. The arrangement of anions in many of these compounds approximates either cubic-or hexagonal-close packing. The observed orientation relationships were always such as to allow the best possible fit between the close-packed planes of starting material and the product. Among the other early workers in the area of inorganic oxycompounds the names of Feitknecht[31,32], Brindley[12], Taylor[11] and Mackay[29] stand out prominently.

7. Oxidation of valentinite, Sb_2O_3, to cervantite, Sb_2O_4

During studies on the polymorphic transformation in antimony trioxide, Sb_2O_3, a serendipitous discovery was made in the author's laboratory that a single crystal of the orthorhombic form of Sb_2O_3, valentinite, could be oxidised to a single crystal of the

higher oxide, cervantite, Sb_2O_4[33]. Further studies, described below, showed that this oxidation is an interesting example of a topotactic reaction. Valentinite belongs to the centrosymmetric orthorhombic space group Pccn. Its structure, determined many years ago by Buerger and Hendricks[34] and subsequently refined by Svensson[35], consists of infinite chains of Sb_4O_6 groups extending along [001], alternate chains in the unit cell running antiparallel. Within the chains, each Sb(III) is bonded to three O atoms and each O to two Sb atoms. There are also weak bonds between Sb of one chain and O of the neighbouring chain. Cervantite belongs to the noncentrosymmetric orthorhombic space group $Pc2_1n$. In the crystal structure, each Sb(V) is linked to six O atoms at the corners of a distorted octahedron[36]. These SbO_6 groups share edges and form corrugated sheets parallel to (010). Adjacent sheets are joined through Sb(III) atoms, which have a one-sided four-fold coordination of O atoms. Projections of the two structures down *a* and *c* axes are given in figs 6 and 7.

Heating of single crystals of valentinite in air around 490°C for more than 8 hours resulted in complete conversion to cervantite. However, by heating for a shorter period, *ca* 4 h, a 'hybrid' crystal containing both phases could be obtained. From an analysis of the rotation and Weissenberg photographs of the latter, it was established that the three crystallographic axes of the reactant and product are individually parallel[33]. That is, $a_{val} \| a_{cerv}$, $b_{val} \| b_{cerv}$ and $c_{val} \| c_{cerv}$. The near equality of corresponding cell parameters may be noted in Table IV.

The close relationship between the two structures could be deduced by comparing the projections down *a* and *c* axes in the appropriate orientations as shown in figs 6 and 7[33]. It can be seen that the relative positions of the atoms belonging to the Sb_4O_6 groups are almost identical in the two structures. One such group, designated Sb(1), O(2), Sb(3), O(4), Sb(5), O(6), Sb(7), O(8), O(9) and O(10) in valentinite (figs 6a and 7a), is clearly seen in both the projections of cervantite (figs 6b and 7b). The only additional O atoms in cervantite are O(11) and O(12). As fig. 7 clearly shows, these O atoms have taken up positions along the empty channels present between neighbouring chains in the valentinite structure. Each O atom bridges two Sb atoms of neighbouring chains along [100] direction. This together with a closing up of chains along [010] results in the chain structure of valentinite being converted to the three-dimensional structure of cervantite.

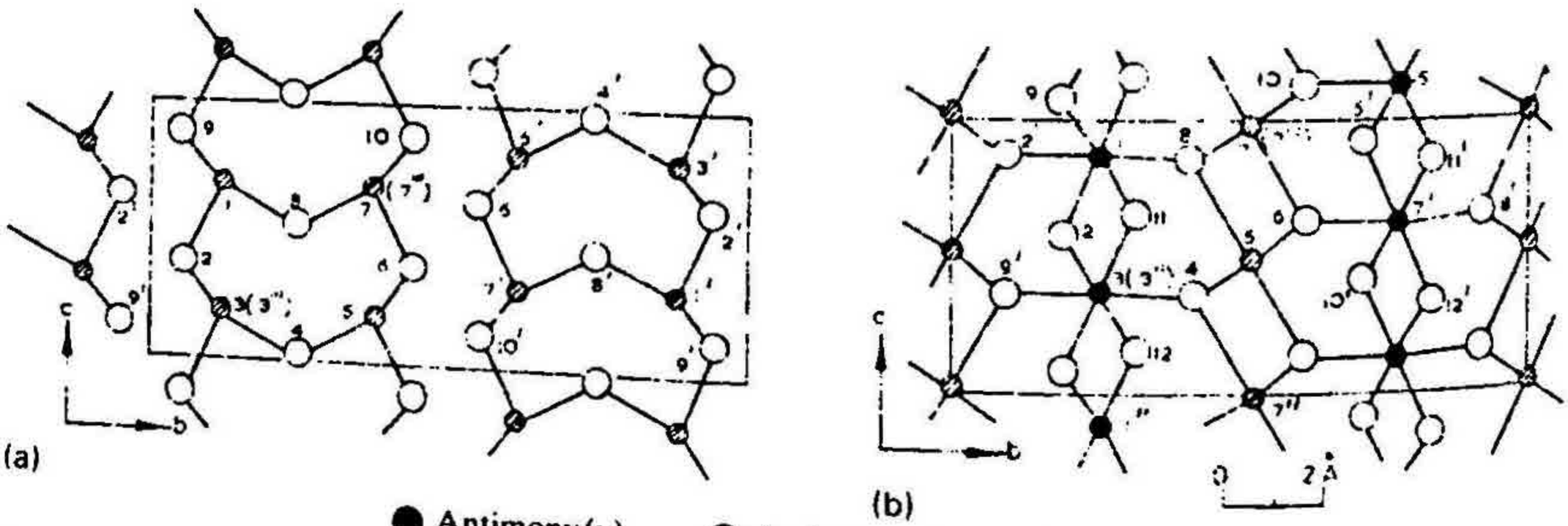

FIG. 6. [100] Projections of (a) valentinite and (b) cervantite (reprinted with permission from ref. 33).

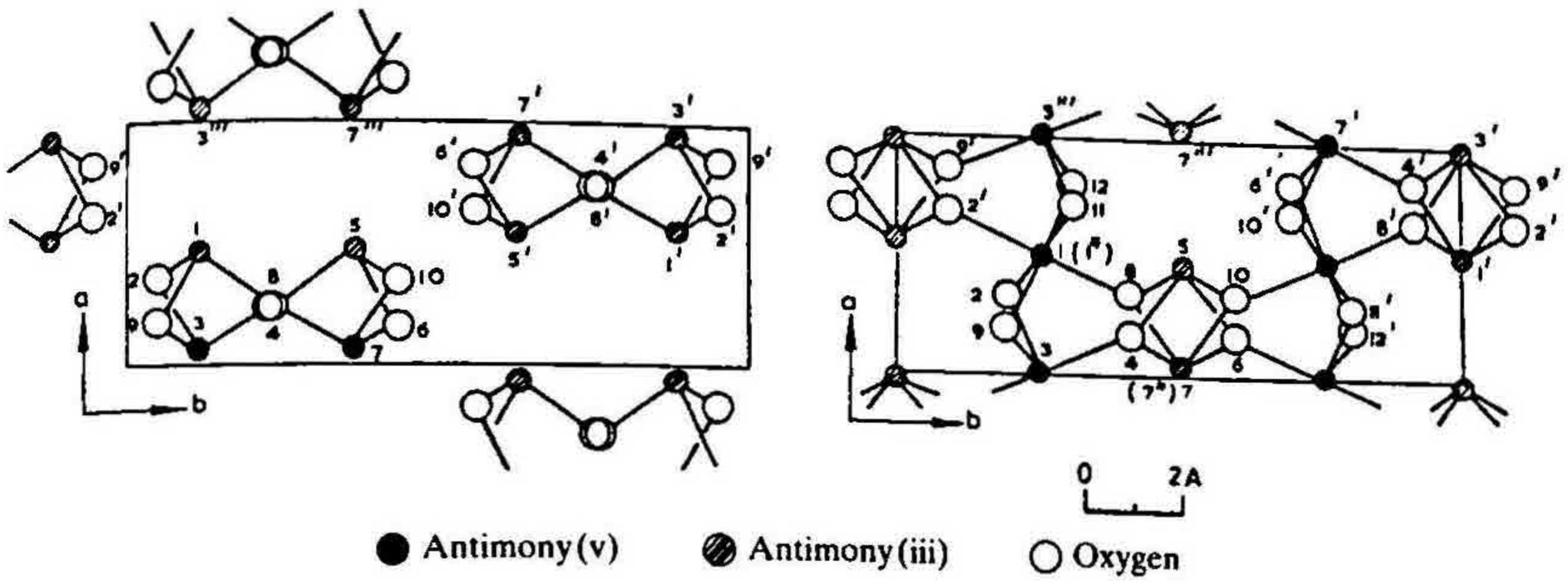

(a) (b)

FIG. 7. [001] Projections of (a) valentinite and (b) cervantite (reprinted from ref. 33 with permission).

The reduction of cervantite to valentinite has also been shown to take place topotactically. Thus, perhaps for the first time ever, a one-to-one correspondence of atomic positions in the two structures could be established. In fact, the shifts of the individual atoms of valentinite in the course of the reaction (< 0.64 Å) have also been calculated[33].

The structural studies have been supplemented by kinetic studies in single crystals using hot-stage microscopy[37]. By very careful experimentation, it has been possible to obtain the rates of the reaction along different crystallographic directions *b* and *c*. The combined results from these two types of studies lead to the conclusion that the diffusion mechanism for the oxidation is governed mainly by structural considerations.

8. Topotactic conversion of aragonite to hydroxyapatite

In recent years increasing attempts are being made to produce prosthetic implants from porous natural bio-materials. Stringent specifications have to be met by bio-materials

Table IV
Crystallographic data for valentinite, Sb_2O_3 and cervantite, Sb_2O_4[33]

Parameter	Sb_2O_3	Sb_2O_4	Relative change
a(Å)	4.914	4.810	−2.1%
b(Å)	12.468	11.76	−5.7%
c(Å)	5.421	5.436	+0.28%
V(Å^3)	332.1	307.5	−7.4%
Space group	Pccn	$Pc2_1n$	
Z	4	4	

+ = Expansion; − = Contraction.

being considered for tooth or bone replacements. Porous solids have the advantage of allowing circulation of body fluids and of increasing the chances of firm attachment to body tissues. Phosphatic material, which are porous, inorganic and sterile, being formed at high temperatures and pressures, are good candidates for this role. Among the most promising starting materials are skeletal corals, consisting of calcium carbonate with the aragonite modification[38]. Metal, ceramic or polymer replicas have been made from suitable corals. However, it has also been possible to transform coral materials directly into hydroxyapatite, $Ca_{10}(PO_4)_6\,(OH)_2$, which forms the inorganic component of bones and teeth. It has been shown by Roy and coworkers that during the hydrothermal reaction, *e.g.*, with ammonium phosphate,

$$10\,CaCO_3 + 6(NH_4)_2\,HPO_4 + 2H_2O \rightarrow$$

aragonite

$$Ca_{10}(PO_4)_6\,(OH)_2 + 6(NH_4)_2\,CO_3 + 4H_2CO_3$$

apatite

Scheme III

the coral structure is preserved due to a topotactic reaction, which is controlled by a two-dimensional structural relationship between the two compounds[39].

In the experimental studies, single crystals of aragonite were treated hydrothermally with phosphate solutions in sealed gold tubes at temperatures of 260–400°C and pressures of *ca* 1 kbar[39]. At low temperatures the reaction was slow, taking 1–3 weeks. The products were analysed by X-ray diffraction, optical and electron microscopy, IR spectroscopy, etc. The apatite formed is not a single crystal, but consists of fibres.

The orthorhombic cell of aragonite can be converted into a pseudohexagonal cell of double size, the basis of which is very similar to that of the apatite structure (Table V). Cell parameter *a* of the pseudohexagonal cell (face diagonal of the orthorhombic cell) is nearly the same as that of the hexagonal apatite; the pseudohexagonal angle is also very close to 120°. The base areas (A*) are also nearly equal. A comparison not only of the unit cells, but also of the crystal structures shows an approximate relationship. The aragonite structure (fig. 8) can be described formally as consisting of calcium channels which occur in the projection as six-membered rings. The CO_3 triangles are situated in these channels. In the apatite structure (fig. 9), we find at the corners of the projected cell the same six-membered calcium rings, which contain hydroxyl ions. Compared to the rings in the aragonite structure, however, these rings are rotated by 30°, thus creating four-membered rings in the centre of the cell. The four-membered rings contain PO_4 tetrahedra. Structurally the correspondence can be described by the formulae:

Aragonite: $Ca_8(CO_3)_6\,(CO_3)_2 = 8CaCO_3$;

Apatite: $Ca_{10}(PO_4)_6\,(OH)_2$.

There exist two more Ca atoms on the trigonal axes of apatite. Therefore, in Scheme III two additional formula weights of $CaCO_3$, *i.e.*, $10CaCO_3$, are needed. Additional

Table V
Relationships of the unit cells of aragonite and apatite[39]

	Symmetry	Cell parameters				Base area
		a(Å)	b(Å)	c(Å)	ν(°)	A* (Å^2)
Aragonite (Alston Moore, England)	Orthorhombic, Pcmn	7.961	4.958	5.739	90	39.5
	Pseudo-hexagonal	9.378	—	5.739	117.0	79.0
Hydroxyapatite (Synthesised from aragonite of Alston Moore + $Ca(H_2PO_4)_2 \cdot H_2O$)	Hexagonal, $P6_3/m$	9.423	—	6.882	120	76.9

support for the structural relationship comes from the experimental fact that in carbonate apatites all OH ions and up to 25% of PO_4 tetrahedra can be replaced by CO_3 triangles.

9. Photodimerization of 2-benzyl-5-benzilidenecyclopentanone and its *p*-bromo derivative

The solid-state photodimerizations of 2-benzyl-5-benzilydenecyclopentanone (BBCP, I) and its *p*-bromo derivative, 2-benzyl-5-*p*-bromobenzylidenecyclopentanone (BpBrBCP, II) (Scheme IV), have been shown by Thomas and coworkers to be topotactic transformations[40]. A crystal of I was mounted on a goniometer head and irradiated with UV radiation ($\lambda > 320$ nm); X-ray photographs were taken after 1.5, 4.5, 21.5 and 65.5 h of irradiation. The dimerization was complete after 65.5 h. Both the monomer and dimer are orthorhombic and the coincidence of the three axes of the dimer with those of the monomer was established from oscillation and Weissenberg photographs. In the case of

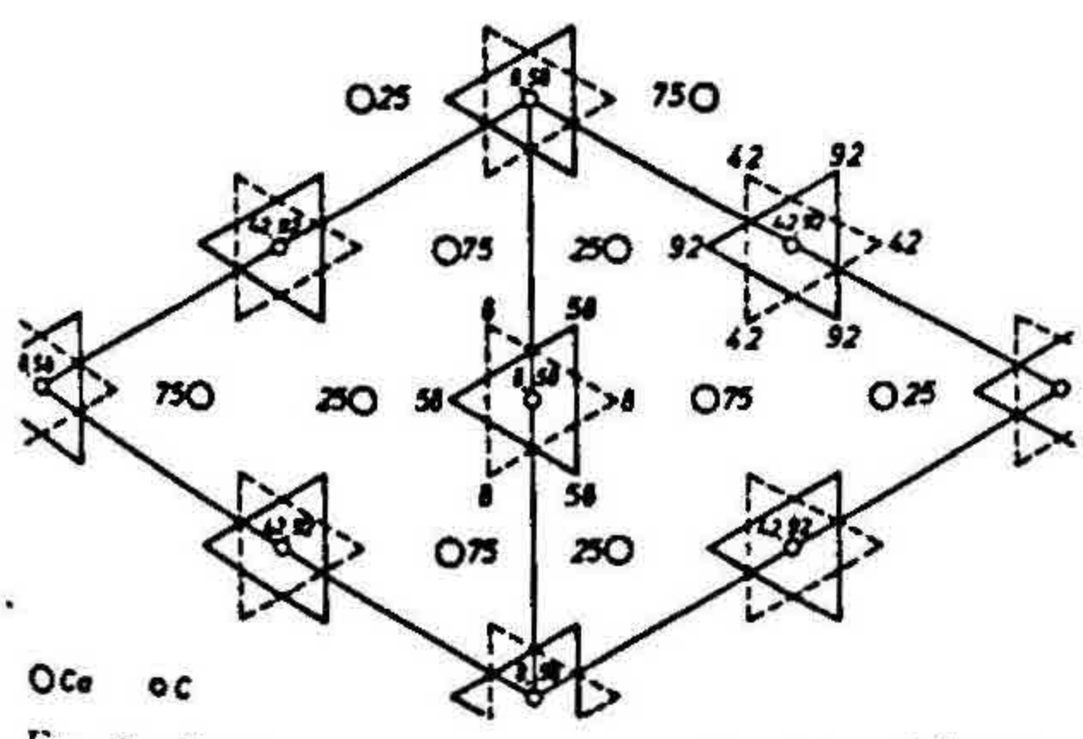

FIG. 8. Crystal structure of aragonite. Pseudohexagonal cell projected along c. Heights are in fractions of 100 (reprinted from ref. 39 with permission).

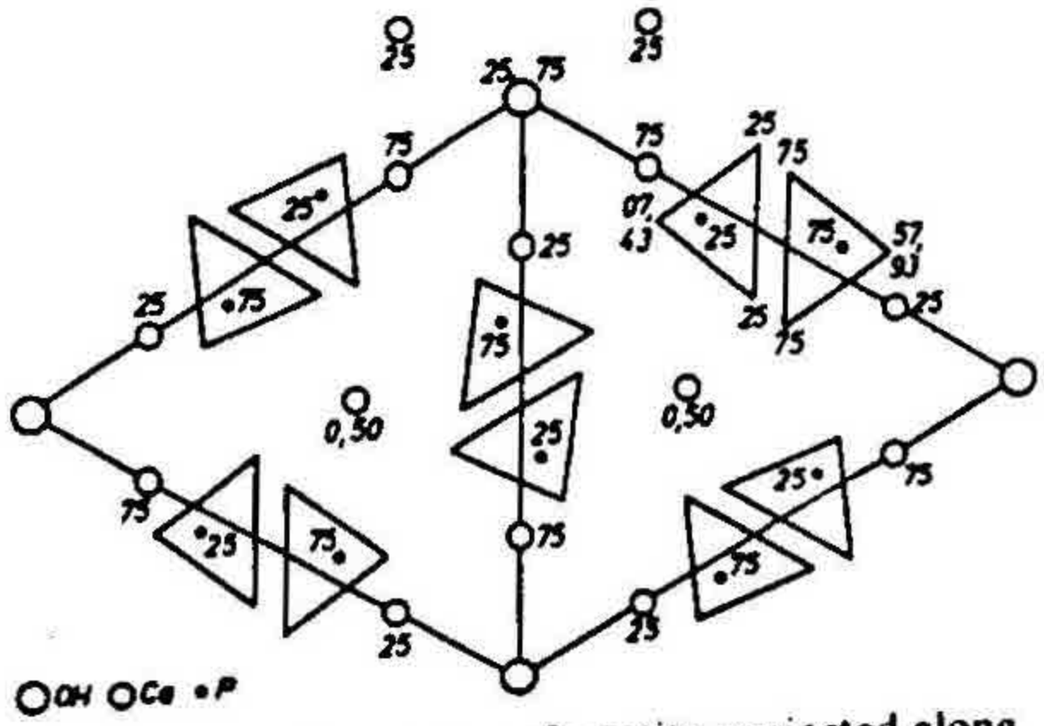

FIG. 9. Crystal structure of apatite projected along c. Heights are in fractions of 100 (reprinted from ref. 39 with permission).

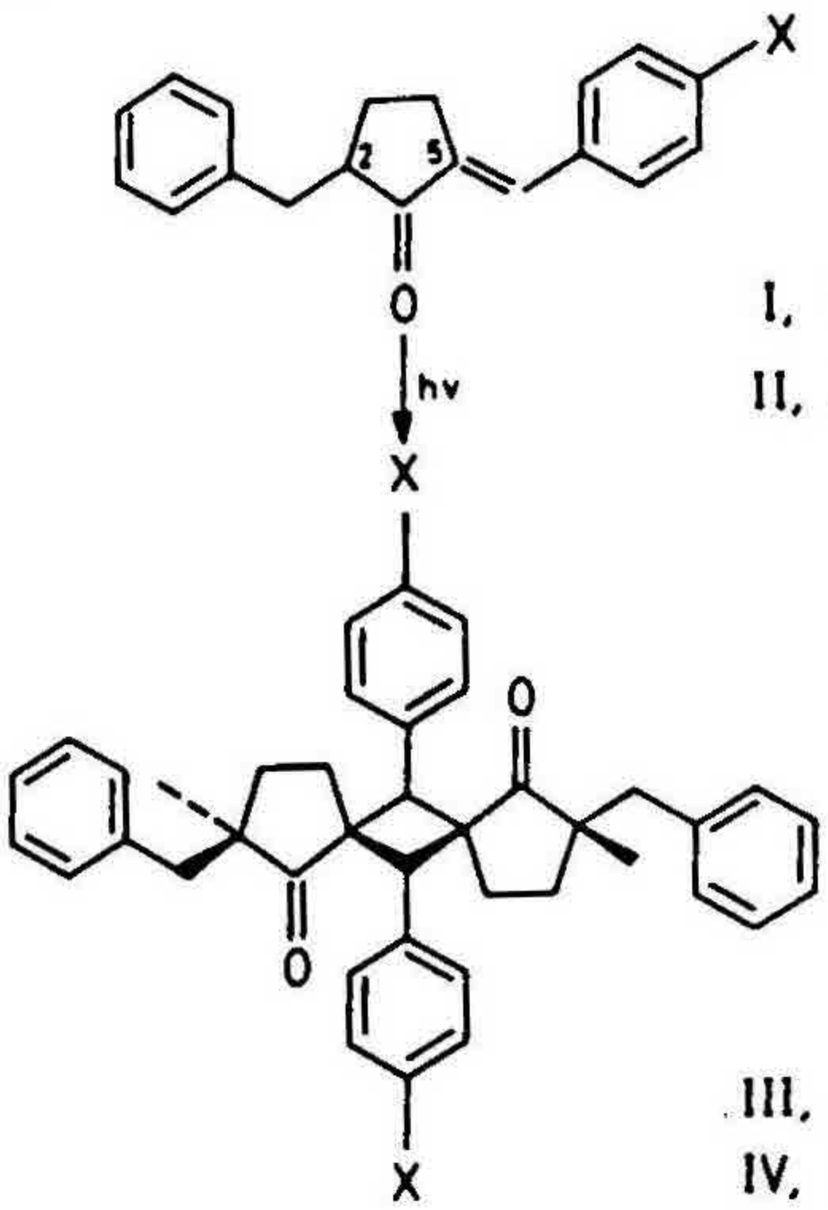

I, X = H
II, X = Br
III, X = H
IV, X = Br

Scheme IV

BpBrBCP(II), exposure to room daylight itself provided a suitably slow conversion rate and yielded single crystals of the product. The cell parameters for the four compounds are listed in Table VI.

Single crystals of the monomer were next irradiated, *in situ*, on an X-ray diffractometer. Accurate cell dimensions were determined at the commencement of the experiment and after each irradiation. The variation in cell parameters was thus monitored during the course of the reaction[41]. The variations were smooth and continuous for both BBCP and BpBrBCP, suggesting that the transformation mechanisms are broadly similar.

Intensity data sets were collected for BBCP monomer(I) and dimer(III), BpBrBCP monomer(II) and also for a crystal of BBCP at two intermediate points of conversion

Table VI
Crystal data for BBCP and BpBrBCP[41]

	BBCP			BpBrBCP		
	Monomer	Dimer	% change	Monomer	Dimer	% change
a(Å)	31.30	31.32	0.06	34.25	32.96	−3.77
b(Å)	10.78	10.81	0.28	10.88	10.27	−5.61
c(Å)	8.69	8.63	−0.69	8.43	8.98	6.52
V(Å^3)	2932	2922	0.34	3141	3040	3.22
Space group	Pbca	Pbca		Pbca	Pbca	
Z	8	4		8	4	

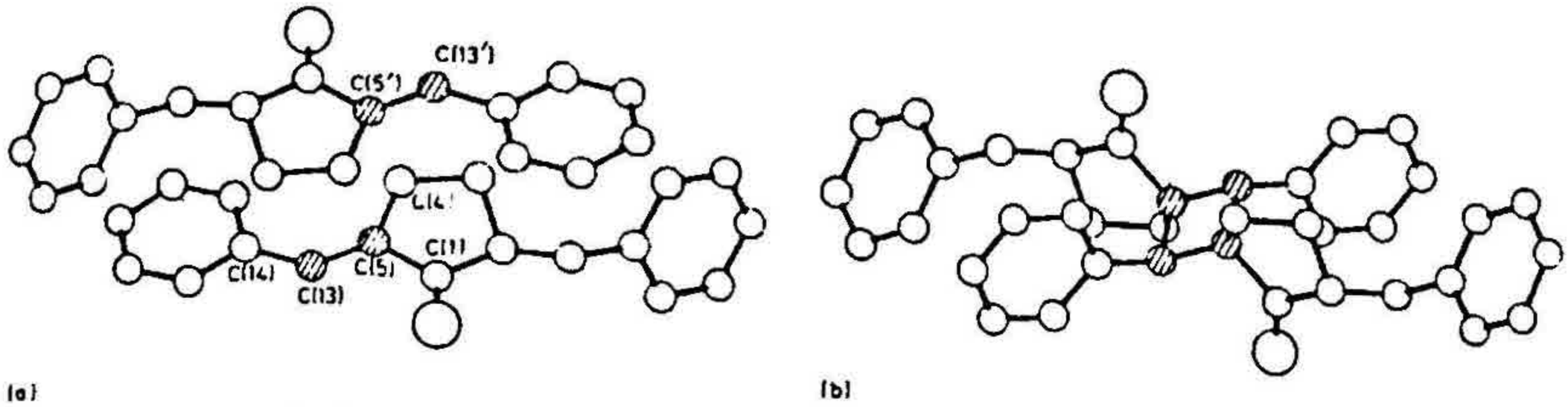

FIG. 10. (a) The projection on (001) of the BBCP monomer structure showing two molecules across a centre of symmetry. (b) The projection on (001) of the BBCP dimer structure (reprinted from ref. 41 with permission).

(approximately 30 and 70%) and the crystal structures solved[42]. (The crystal structure of BpBrBCP dimer(IV) is already known). In the case of the two monomers, I and II, which are isomorphous, the principal packing modes are the same, the molecules forming incipient dimer pairs across centres of symmetry (fig. 10a). The intermolecular distances between double bonds in the centrosymmetrically related molecules, *i.e.*, C(5)–C(13'), are 4.166 and 3.798 Å and the ethylenic plane-to-plane distances, C(1)–C(5)–C(4)–C(13)–C(14), are 3.80 and 3.60 Å, respectively. Consequent upon UV irradiation these pairs of molecules react topochemically to yield centrosymmetric photodimers (fig. 10b). Thus the reaction is not only single crystal to single crystal, but also topochemically controlled. As in the example in Section 7, the atomic shifts during the reaction have been calculated. It is noteworthy that even though some of the atoms shift by more than 1 Å, the single crystallinity is not lost. The conversions are in a literal sense diffusionless. In the case of the structures of the partly converted 'mixed crystals', the R values are comparatively high, as to be expected. The results suggest that the intermediate-phase crystals cannot be represented by a simple homogeneous solid solution model. This study represents one of the few cases where, using the X-ray crystallographic technique, it was possible to view simultaneously the reactant and product molecules as the chemical reaction proceeded.

10. Concluding remarks

Chemical reactivity studies have generally focussed on two states of matter, *viz.*, the solution and the gas phases, relying on the premise that reactions require mobility of molecules. A common view among chemists and even crystallographers is that a crystal is made up of frozen chemical entities, that can utmost undergo very small translational or librational motions. There are, however, a large number of cases where this 'still-life' picture does not apply. As seen in the examples cited in earlier sections, molecules in highly condensed media can display a selectivity which is unimaginable in solution-or gas-phase experiments. Perhaps the main reason why solid-state reactions are still regarded as more or less chemical curiosities is the experimental difficulty in identifying reactive crystals. However, with a deeper understanding of short contacts, packing effects and of topochemistry, such reactions can be recognised and exploited in chemistry. It is in this context that X-ray crystallography assumes a very important role.

This review is not primarily intended for the specialist in solid-state chemistry, but rather for the practising chemist and X-ray crystallographer. Its purpose is to bring home to both groups of scientists, the vast potential of X-ray structure analysis for understanding atomic/molecular motions, phase transitions and reactions in the crystal, rather than merely being a tool for elucidating molecular geometry.

Acknowledgement

The author thanks K. Vyas for useful discussions.

References

1. Lotgering, F. K. — *J. Inorg. Nucl. Chem.*, 1959, **9**, 113–123.
2. Schmidt, G. M. J. — *Pure Appl. Chem.*, 1971, **37**, 647–678.
3. Thomas, J. M. — *Phil. Trans. R. Soc.* (*Lond.*), 1974, **277**, 251–286.
4. Thomas, J. M. — *Pure Appl. Chem.*, 1979, **51**, 1065–1082.
5. Paul, I. C. and Curtin, D. Y. — *Acc. Chem. Res.*, 1973, **6**, 217–225.
6. Paul, I. C. and Curtin, D. Y. — *Science*, 1975, **187**, 19–26.
7. Desiraju, G. R. — *Indian J. Chem. Edn*, 1980, **7**(1), 1–8.
8. Desiraju, G. R. — *Endeavour*, 1984, **8**, 201–206.
9. Green, B. S., Arad-Yellin, R. and Cohen, M. D. — In *Topics in stereochemistry*, Eliel, E. (ed.), John Wiley, 1986, Vol. 16, pp. 1–154.
10. Ramamurthy, V. and Venkatesan, K. — *Chem. Rev.*, 1987, **87**, 433–481.
11. Dent Glasser, L. S., Glasser, F. P. and Taylor, H. F. W. — *Q. Rev.* (*Lond.*), 1962, **16**, 343–360.
12. Brindley, G. W. — In *Progress in ceramic science*, Pergamon Press, Oxford, 1963, Vol. 3, pp. 1–56.
13. Bernal, J. D. and Mackay, A. L. — *Tschermaks. Mineral. Petrogr. Mitt.*, 1965, **10**, 331–340.
14. Gougoutas, J. Z. — *Pure Appl. Chem.*, 1971, **27**, 305–325.
15. Dasgupta, D. R. — *Indian J. Earth Sci.*, 1974, **1**, 60–72.
16. Manohar, H. — In *Solid state chemistry*, Rao, C. N. R. (ed.), Marcel Dekker, 1974, pp. 95–131.
17. Manohar, H. — *J. Indian Inst. Sci.*, 1975, **57**, 468–488.
18. Cohen, M. D. and Schmidt, G. M. J. — *J. Chem. Soc.*, 1964, 1996–2100.

19. ELGAVI, A., GREEN, B. S. AND SCHMIDT, G. M. J. — *J. Am. Chem. Soc.*, 1973, **95**, 2058–2059.

20. ADDADI, L., VAN MIL, J. AND LAHAV, M. — *J. Am. Chem. Soc.*, 1982, **104**, 3422–3429.

21. GORDON, A. J. — *Tetrahedron*, 1967, **23**, 863–870.

22. VYAS, K. AND MANOHAR, H. — *Mol. Cryst. Liq. Cryst.*, 1986, **137**, 37–43.

23. VYAS, K., MOHAN RAO, V. AND MANOHAR, H. — *Acta Crystallogr.*, 1987, **C43**, 1197–1204.

24. DUNITZ, J. D. — *X-ray analysis and the structure of organic molecules*, Cornell University Press, 1979, Ch. 7 and references therein.

25. SUKENIK, C. N., BONAPACE, J. A. P., MANDEL, N. S., LAU, P.-Y., WOOD, G. AND BERGMAN, R. G. — *J. Am. Chem. Soc.*, 1977, **99**, 851–858.

26. ARJUNAN, P., RAMAMURTHY, V. AND VENKATESAN, K. — *J. Org. Chem.*, 1984, **49**, 1765–1769.

27. DESIRAJU, G. R. — *Indian J. Chem. Edn*, 1980, 7(2), 1–6 and references therein.

28. BERNAL, J. D., DASGUPTA, D. R. AND MACKAY, A. L. — *Nature*, 1957, **180**, 645–647.

29. MACKAY, A. L. — In *Reactivity of solids*, DeBoer, J. H. (ed.), Elsevier, 1961, p. 571.

30. DENT GLASSER, L. S., GLASSER, F. P. AND TAYLOR, H. F. W. — *Q. Rev. (Lond.)*, 1962, **16**, 343–360, and references therein.

31. FEITKNECHT, W. AND LEHMANN, H. W. — *Helv. Chim. Acta*, 1959, **42**, 2035–2039.

32. FEITKNECHT, W., OSWALD, H. R. AND FEITKNECHT-STEINMANN, U. — *Helv. Chim. Acta*, 1960, **43**, 1947–1950.

33. GOPALAKRISHNAN, P. S. AND MANOHAR, H. — *Pramāna*, 1974, **3**, 277–285.

34. BUERGER, M. J. AND HENDRICKS, S. B. — *Z. Kristallogr.*, 1937, **98**, 1–30.

35. SVENSSON, C. — *Acta Crystallogr.*, 1974, **B30**, 458–461.

36. GOPALAKRISHNAN, P. S. AND MANOHAR, H. — *Cryst. Str. Comm.*, 1975, **4**, 203–206.

37. GOPALAKRISHNAN, P. S. AND MANOHAR, H. — *J. Solid St. Chem.*, 1976, **16**, 301–306.

38. ROY, D. M. AND LINNEHAN, S. K. — *Nature*, 1974, **247**, 220–222.

39. EYSEL, W. AND ROY, D. M. — *Z. Kristallogr.*, 1975, **141**, 11–24.

40. NAKANISHI, H., JONES, W. AND THOMAS, J. M. — *Chem. Phys. Lett.*, 1980, **71**, 44–48.

41. NAKANISHI, H., JONES, W., THOMAS, J. M., HURSTHOUSE, M. B. AND MOTEVALLI, M. — *J. Chem. Soc.*, (*Chem. Comm.*), 1980, 610–611.

42. NAKANISHI, H., JONES, W., THOMAS, J. M., HURSTHOUSE, M. B. AND MOTEVALLI, M. — *J. Phys. Chem.*, 1981, **85**, 3636–3642.